

PACS numbers: 63.10.+a, 63.20.D-, 63.20.dh, 63.22.Np, 63.22.Rc

Study of Lattice Vibrations of the Stanene Along Highly Symmetry Directions

Kamlesh Kumar, M. Imran Aziz, and Rahul Kumar Mishra

*Physics Department,
Shibli National Postgraduate College,
Azamgarh, India*

Lattice vibrational properties of single-layer two-dimensional honeycomb lattices of stanene is one of the important areas of research due to their potential for integration into next-generation electronic industry. Stanene exhibits ductile nature and hence could be easily incorporated with existing technology in semiconductor industry on substrates in comparison to graphene. We focus on the lattice vibrational properties of stanene, try to understand them from its honeycomb, and buckled lattice structures. At present, we find the vibrational frequencies at Γ point along symmetry directions using the adiabatic bond-charge model with the help of Python program. The acoustical and optical contributions to the phonon frequencies are also discussed. We hope that phonon frequencies along Γ - M direction of stanene 2D materials will have reasonably similar result as obtained by other researchers.

Коливні властивості ґратниці одношарових двовимірних стільникоподібних ґратниць станену є одним з важливих напрямів досліджень завдяки їхньому потенціалу для інтеграції в електронну промисловість наступного покоління. Станен демонструє пластичний характер і, отже, може бути легко включений з існуючими технологіями в напівпровідниковій промисловості на підкладинки у порівнянні з графеном. Ми зосереджуємося на коливних властивостях ґратниці станену та намагаємося зрозуміти їх з його стільникоподібних і покороблених ґратнице-вих структур. В даний час ми знаходимо коливні частоти в точках Γ вздовж напрямків симетрії за допомогою адіабатичного моделю зарядів на зв'язках за допомогою мови програмування Python. Також обговорюється акустичний і оптичний внески у фононні частоти. Сподіваємося, що фононні частоти вздовж напрямку Γ - M станенових 2D-матеріалів матимуть достатньо аналогічний результат як одержаний іншими дослідниками.

Key words: bond-charge model, lattice vibrations of stanene, phonon fre-

quencies.

Ключові слова: модель зарядів на зв'язках, коливання ґратниці станену, фононні частоти.

(Received 5 August, 2022)

1. INTRODUCTION

The use of phenomenological models in the study of the vibrational properties of stanene allows a complete and straightforward description of the phonon dispersion and phonon eigenvectors in the whole Brillouin zone (BZ) with clear physical ingredients and a small computational effort. Stanene, the other group-IV 2D material, with honeycomb and buckled lattice structures has been discovered by epitaxial growth on substrates [1, 2]. The lattice vibrations are responsible for the characteristic properties of solid such as phonon properties, phonon group velocities, phonon scattering mechanism, thermal conductivity, elastic and dielectric properties, *etc.* The atoms in a solid are executing oscillations about their equilibrium positions with energy governed by the temperature of the solid; such oscillations in crystals are called the lattice vibrations. The vibration of the atoms depends on the interatomic interaction within the crystal. The adiabatic bond-charge method (BCM) was originally developed by Weber [3]. Very recently, the researchers have investigated that, among group-IV elements, there are not only graphene but also silicene, germanene and stanene as stable honeycomb structures with 2D nanostructure [4, 5]. To determine the vibrational frequencies and the corresponding modes, one needs to calculate the eigenvalues and the eigenvectors of the so-called dynamical matrix, which can be obtained from the interatomic-interaction potential [7–10]. If the dynamical matrix is known, the eigenvalues' problem is straightforward. There have been several theoretical attempts to understand the lattice vibrations and thermal properties of stanene [11–13], which usually employing the force-constants' model, the rigid-ions' model, the rigid-shells' model, the dipole approximation, *etc.*, but bond-charge model is showing best results for the IV-th group of semiconductors.

The total energy per honeycomb-structure unit cell is as follows:

$$\begin{aligned} \Phi_{total} = & 3[\varphi_{ii}(t) + \varphi_1(r_1) + \varphi_2(r_2)] - \\ & - a_M^{eff} \frac{(3Z)^2 e^2}{\epsilon t} + 3[V_{bb}^1 + V_{bb}^2 + \psi_1(r_{bb}^1) + \psi_2(r_{bb}^2)] + \frac{1}{2} h\omega_j(\mathbf{q}). \end{aligned} \quad (1)$$

The Fourier transform of modified adiabatic bond-charge model

equations of motion is as follows:

$$m\omega^2 u = \left[R + 9 \frac{(Ze)^2}{\varepsilon} C_R \right] u + \left[T - 6 \frac{(Ze)^2}{\varepsilon} C_T \right] v. \quad (2)$$

The condition for the non-trivial solutions for this wave equation leads to the characteristic or secular equation:

$$|D^{eff}(\mathbf{q}) - \omega^2(\mathbf{q})mI| = 0, \quad \omega = \omega_j(\mathbf{q}), \quad j = 1, 2, 3, \dots, 2n. \quad (3)$$

This secular equation of 2×2 dimensions can be further extended as

$$-\omega^2 mIU = [D(0,0) + D(0,1)D(1,1)^{-1}D(1,0)]U, \quad (4)$$

where

$$D(0,0) = \begin{pmatrix} D_{xx}(0,0) & D_{xy}(0,0) \\ D_{yx}(0,0) & D_{yy}(0,0) \end{pmatrix}, \quad (5)$$

$$D(1,0) = \begin{pmatrix} D_{xx}(1,0) & D_{xy}(1,0) \\ D_{yx}(1,0) & D_{yy}(1,0) \end{pmatrix}, \quad (6)$$

$$D(0,1) = \begin{pmatrix} D_{xx}(0,1) & D_{xy}(0,1) \\ D_{yx}(0,1) & D_{yy}(0,1) \end{pmatrix}, \quad (7)$$

$$D(1,1) = \begin{pmatrix} D_{xx}(1,1) & D_{xy}(1,1) \\ D_{yx}(1,1) & D_{yy}(1,1) \end{pmatrix}. \quad (8)$$

The elements of dynamical matrix are defined as

$$D_{\alpha\beta}(k, k')(\mathbf{q}) = \sum_{l'} \Phi_{\alpha\beta}(l' - l; k k') \exp(i\mathbf{q} \cdot \mathbf{r}(lk, l'k')). \quad (9)$$

The above-mentioned equation in matrix form is solved by MATLAB program, and the result is investigated along hexagonal Brillouin zone with symmetry points $\Gamma(0,0)$, $M(2\pi/(a\sqrt{3}), 0)$.

The vibrational frequencies along symmetry line Γ - M with coupling constant $\gamma_j = 8.4 \cdot 10^{-3} \gamma$ for stanene are deduced as follow:

$$\omega_1^2 = \gamma_j \left[1 - \cos \left(\frac{\sqrt{3}}{2} q_y a \right) \right], \quad (10)$$

$$\omega_2^2 = 3\gamma_j \left[1 - \cos \left(\frac{\sqrt{3}}{2} q_y a \right) \right], \quad (11)$$

$$\omega_3^2 = \gamma_j \left[\frac{3}{2} - \frac{5}{4} - \cos \left(\frac{\sqrt{3}}{2} q_x a \right) \right], \quad (12)$$

$$\omega_4^2 = \gamma_j \left[\frac{3}{2} + \frac{5}{4} + \cos \left(\frac{\sqrt{3}}{2} q_x a \right) \right], \quad (13)$$

$$\omega_5^2 = 0, \quad (14)$$

$$\omega_6^2 = 3\gamma_j. \quad (15)$$

3. PHONON-DISPERSION CURVE

Using the phonon dispersion at $a = 4.67 \text{ \AA}$, we computed the different modes as shown in Table with help of Python program.

The phonon-dispersion relations have been computed by solving the secular equation for the six vibrational frequencies corresponding to the phonon wave vectors along the principal symmetry direction $\Gamma-M$.

The phonon-dispersion curves have been obtained by plotting the vibrational frequencies (ω) against the wave vector (\mathbf{q}) with the help of Python program, and following points are investigated from the careful analysis of phonon-dispersion curve for stanene along high-

TABLE. Calculated phonon frequencies (THz) for stanene.

Wave vector \mathbf{q}	Transverse-acoustic mode (TA)	Longitudinal-acoustic mode (LA)	Z-direction-acoustic mode (ZA)	Longitudinal-optical mode (LO)	Z-direction-optical mode (ZO)	Transverse-optical mode (TO)
0.0	0.000000	0.000000	3.964215	5.803016	0	5.190376
0.1	0.757665	1.312314	4.035970	5.753342	0	5.190376
0.2	1.490915	2.582341	4.235307	5.608224	0	5.190376
0.3	2.176125	3.769159	4.522225	5.379543	0	5.190376
0.4	2.791214	4.834525	4.848286	5.087644	0	5.190376
0.5	3.316363	5.744109	5.168488	4.762010	0	5.190376
0.6	3.734650	6.468604	5.446339	4.441552	0	5.190376
0.7	4.032598	6.984664	5.654807	4.172907	0	5.190376
0.8	4.200604	7.275659	5.775818	4.003739	0	5.190376

symmetry direction. The dispersion of the longitudinal phonons exhibits oscillatory behaviour in large wave-vector region. In contrast, for the ω - \mathbf{q} curves of the transverse phonons, the oscillatory behaviour seems quite insignificant for the higher \mathbf{q} value. This indicates that the transverse phonons undergo large thermal motion than do for the longitudinal phonons. The ω - \mathbf{q} curves for the longitudinal phonons attain maxima at the higher \mathbf{q} value.

Figure shows the calculated phonon dispersions for stanene, which are in agreement with previous works [15–17]. Similar to other 2D materials, the longitudinal acoustic (LA) and transverse acoustic (TA) branches for the group-IV materials are linear near the Γ point [14]. Three-body interactions have influenced LO and TO branches much more than the acoustic LA and TA branches in this group-IV semiconductor 2D material. For wave vectors along the $\Gamma(0,0)$ - $M(2\pi/(a\sqrt{3}),0)$ symmetry direction, both of the LA and TA modes are degenerate. There is apparent near crossing in mid points, called anti-crossing of the LO and TO modes along the $\Gamma(0,0)$ - $M(2\pi/(a\sqrt{3}),0)$ direction. This phenomenon is dominant in stanene. In high-symmetry situations, it is possible to separate LO modes from TO modes.

Note that the main characteristic of the dispersion curve is a separation of the optical and acoustic modes' frequencies across the range of wave vectors. This is because of the association of optical vibrations with electric moments. Indeed, the transverse modes show a separation of the optical and acoustic modes, but there is a crossing of the LA and TA modes at 3.8788 THz and 4.4848 THz. Optical vibrations are important chiefly for the stanene owing to the strong electric moments associated with motion. Lattice vibrations with wave vector ended in $M(2\pi/(a\sqrt{3}),0)$ are showing LO modes moving in opposite directions parallel to $M(2\pi/(a\sqrt{3}),0)$, and

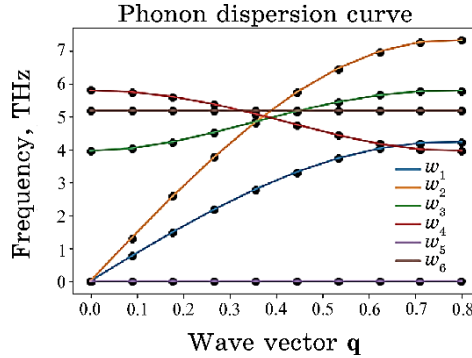


Fig. Phonon frequencies along the high-symmetry direction Γ - M for stanene.

the TO modes moving in opposite directions perpendicular to $M(2\pi/(a\sqrt{3}), 0)$. At $\Gamma[0,0]$, the both types of motion become exactly equivalent; in this case, the LO and TO frequencies would be equal at 5 THz. But as shifting from $[0,0]$ to $M(2\pi/(a\sqrt{3}), 0)$, the long-wavelength optical modes generate electric fields, which are either parallel or perpendicular to the direction of propagation of the optical mode and will have a significant effect on the frequency of the mode. The dispersion relations along symmetry line show the behaviour, as, at $M-K$ points, all four branches are non-degenerate. It should be also noticed that the LA branch (highest longitudinal phonon branch at the M point) remains the same with or without the LO-LA coupling, which is similar to the LO branch.

4. RESULTS

We study the relation between structural and vibrational/thermal properties. We computed lattice dynamical model (BCM) based on calculations of the phonon spectrum with the help of MATLAB. Based on these calculations, using the quasi-harmonic approximation (QHA), we obtained the vibrational frequencies of stanene 2D materials. For the dynamical properties, we need a large unit cell to treat the long-range interaction, which is important for the long wavelength, low frequency phonons near Γ . The vibrational and thermal properties are computed using Python-QHA script.

The calculated phonon dispersion relations along high-symmetry lines within the Brillouin zone are shown in Figure. The dispersion lines are similar due to the honeycomb lattice structures. The acoustic and optical modes along Z direction (ZA and ZO) do not couple with other phonon modes, resulting in crossings of dispersion lines for stanene along high-symmetry direction because of larger buckling. This results in the development of phonon band gaps and the decrement in phonon group velocity. Further, both of them reduce effectively the phonon thermal conductivity. Interestingly, the large buckling in stanene results in a larger Γ point ZO frequency for stanene, and the ZA mode is very low near Γ points. This means that the applied strain should be small enough, otherwise harmonic approximation is not valid anymore.

5. CONCLUSION

In this paper, we have systematically reported phonon-dispersion curves, combined density of states for stanene. Based on overall fair agreement, it may be concluded that, in the present model, three types of interactions: (i) Coulomb interactions, (ii) short-range cen-

tral force interactions, and (iii) a rotationally invariant Keating-type bond-bending interaction depending on angle are adequately capable to describe the lattice dynamics of stanene [15–18]. The inclusion of van der Waals interaction (vWI) [5] has influenced both the longitudinal and transverse optical modes much more than acoustic branches.

The agreement between theory and experimental data at Γ point is also excellent.

Another striking feature of the present model is noteworthy from the excellent reproduction of almost all branches. The computed phonon-dispersion curves displayed in Figure show that the inclusion of zero-point energy has improved the results. Here, in this paper, lattice vibrational properties of stanene are compared with other researchers. The theoretical predictions achieved for the vibrational frequencies of stanene are in reasonably good agreement with other researchers [19, 21]. The stanene has very high Grüneisen parameter and low group velocity [22], thereby, indicating significantly high harmonicity in this material.

ACKNOWLEDGEMENTS

The authors are grateful to the computer centre, S.N.C., Azamgarh for computational assistance. They are also indebted to Prof. R. S. Singh, DDU Gorakhpur University, for many useful discussions.

REFERENCES

1. A. C. Ferrari, F. Bonaccorso, V. Fal'ko, K. S. Novoselov, S. Roche, P. Bøggild, S. Borini, F. H. Koppens, V. Palermo, N. Pugno et al., *Nanoscale*, **7**: 4598 (2015).
2. K. S. Novoselov, V. I. Fal'ko, L. Colombo, P. R. Gellert, M. G. Schwab, and K. Kim, *Nature*, **490**: 192 (2012); <https://doi.org/10.1038/nature11458>
3. W. Weber, *Phys. Rev. B*, **15**: 4789 (1977); <https://doi.org/10.1103/PhysRevB.15.4789>
4. K. C. Rustagi and W. Weber, *Sol. Stat. Comm.*, **18**: 673 (1976).
5. M. I. Aziz, *PhD Thesis* (Jaunpur: V.B.S.P.U.: 2010).
6. R. K. Singh, *Physics Reports (Netherland)*, **85**: 259 (1982).
7. A. A. Maradudin, E. W. Montroll, G. H. Weiss, and I. P. Ipatova, *Theory of Lattice Dynamics in the Harmonic Approximation. Series 'Solid State Physics'* (Eds. H. Ehrenreich, F. Seitz, and D. Turnbull) (New York: Academic Press: 1971), vol. **3**.
8. P. BruÈesch, *Phonons: Theory and Experiments I (Lattice Dynamics and Models of Interatomic Forces). Springer Series 'Solid State Science'* (Eds. M. Cardona, P. Fulde, and H.-J. Queisser) (Berlin–Heidelberg–New York: Springer-Verlag: 1982), vol. **34**.
9. S. P. Hepplestone and G. P. Srivastava, *Appl. Phys. Lett.*, **87**: 231906 (2005);

- <https://doi.org/10.1063/1.2138790>
10. S. P. Hepplestone and G. P. Srivastava, *Nanotechnology*, **17**, No. 13: 3288 (2006); [doi:10.1088/0957-4484/17/13/035](https://doi.org/10.1088/0957-4484/17/13/035)
 11. Seymour Cahangirov, Hasan Sahin, Guy Le Lay, and Angel Rubio, *Introduction to the Physics of Silicene and Other 2D Materials* (Springer: 2016).
 12. M. Maniraj, B. Stadtmüller, D. Jungkenn, M. Düvel, S. Emmerich, W. Shi, J. Stöckl, L. Lyu, J. Kollamana, Z. Wei, A. Jurenkow, S. Jakobs, B. Yan, S. Steil, M. Cinchetti, S. Mathias, and M. Aeschlimann, *Communications Physics*, **2**, Article number 12 (2019).
 13. Sumit Saxena, Raghvendra Pratap Chaudhary, and Shobha Shukla, *Scientific Reports*, **6**: 31073 (2016).
 14. Gour P. Dasa, Parul R. Raghuvanshi, and Amrita Bhattacharya, *9th International Conference on Materials Structure and Micromechanics of Fracture Phonons and Lattice Thermal Conductivities of Graphene Family* (2019), vol. **23**, p. 334.
 15. Md. Habibur Rahman, Md. Shahriar Islam, Md. Saniul Islam, Emdadul Haque Chowdhury, Pritom Bose, Rahul Jayan, and Md. Mahbubul Islam, *Physical Chemistry Chemical Physics*, **23**: 11028 (2021).
 16. Bo Peng, Hao Zhang, Hezhu Shao, Yuchen Xu, Xiangchao Zhang, and Heyuan Zhu, *Scientific Reports*, August (2015).
 17. Wu, Liyuan Lu, Pengfei Bi, Jingyun Yang, Chuanghua Song, Yuxin Guan, Pengfei Wang, and Shumin, *Nanoscale Research Letters*, **11**: 525 (2016).
 18. Bo Peng, Hao Zhang, Hezhu Shao, Yuanfeng Xu, Gang Ni, Rongjun Zhang, and Heyuan Zhu, *Phys. Rev. B*, **94**: 245420 (2016).
 19. Bo Peng, Hao Zhang, Hezhu Shao, Yuchen Xu, Xiangchao Zhang, and Heyuan Zhu, *Sci. Rep.*, **6**: 20225 (2016).
 20. Kamlesh Kumar and Mohammad Imran Aziz, *American Journal of Nanosciences*, **8**, Iss. 1: 12 (2022); [doi:10.11648/j.ajn.20220801.12](https://doi.org/10.11648/j.ajn.20220801.12)
 21. Xu-Jin Ge, Kai-Lun Yao, and Jing-Tao Lü, *Phys. Rev. B*, **94**: 165433 (2016).
 22. Kamlesh Kumar, M. Imran Aziz, and Nafis Ahmad, *IJSRST*, **9**, No. 2: 323 (2022).
 23. Kamlesh Kumar, Mohammad Imran Aziz, and Khan Ahmad Anas, *American Journal of Nanosciences*, **8**, Iss. 2: 13 (2022); [doi:10.11648/j.ajn.20220802.11](https://doi.org/10.11648/j.ajn.20220802.11)